

# A decrease in pH downstream from the hydroelectric dam in relation to the carbon biogeochemical cycle

Baoli Wang · Cong-Qiang Liu · Fushun Wang ·  
Xiao-Long Liu · Zhong-Liang Wang

Received: 7 April 2014 / Accepted: 5 October 2014 / Published online: 16 October 2014  
© Springer-Verlag Berlin Heidelberg 2014

**Abstract** To better understand the decreases observed in pH levels downstream from the associated hydroelectric dam, the impounded Wujiang River in Southwest China was investigated. Study results indicate that the average pH decrease from upstream to downstream of the hydroelectric dam could be up to 0.47 units, and pH differences were particularly apparent during water thermal stratification. Notably, pH was controlled by  $[\text{CO}_2]/[\text{CO}_3^{2-}]$  ratios in this impounded river. The decrease in  $[\text{CO}_2]/[\text{CO}_3^{2-}]$  ratios and associated increases in pH at the surface of the reservoirs were mainly due to the prevalence of photosynthesis, while the reverse phenomenon was observed at the bottom due to respiration. The evidence from  $\delta^{13}\text{C}_{\text{DIC}}$  clearly demonstrated these processes. The increase in phytoplankton biomass enhanced this pH decrease, while dissolved organic carbon had limited impacts on the pH variation. The decrease in pH downstream from the hydroelectric dam resulted from the development of pH

stratification in the water profile and the dam operations that release bottom waters for hydropower generation. Consequently, the cascade in hydropower development could increase the risk of river acidification.

**Keywords** pH decrease · Eutrophication · Hydroelectric dam · Phytoplankton · Wujiang River

## Introduction

A river is the main conduit for the transport of material from land to the ocean, and its natural state is increasingly being disturbed by human activities. Dam construction, one of the most significant events of such human disturbance, slows water flow thereby increasing water residence time (Vorosmarty et al. 1997). This may further lead to increases in water temperature and nutrient load and, subsequently, algal blooms in the impounded waters due to eutrophication (e.g., Wang et al. 2013; Humborg et al. 1997). As a result, ecosystems of the impoundment shift from river-type heterotrophy to lake-type autotrophy. With these changes, the biogeochemical cycle in the original river is modified and, as such, the carbon geochemical behavior is significantly changed by dam construction (Peng et al. 2014).

A decrease in pH downstream from the hydroelectric dam has been observed (Wang et al. 2014). A pH decrease can cause water acidification and become a serious threat to aquatic ecosystem (e.g., Burns et al. 2008). Traditional knowledge about river acidification is the result of excessive anthropogenic  $\text{SO}_2$  emissions (Larssen et al. 2006; Stoddard et al. 1999). Therefore, widespread recovery about this acidification may occur following considerable  $\text{SO}_2$  emission abatement (Duan et al. 2011; Stoddard et al.

---

B. Wang (✉) · C.-Q. Liu  
State Key Laboratory of Environmental Geochemistry, Institute of Geochemistry, Chinese Academy of Sciences, 46 Guanshui Road, Guiyang 550002, Guizhou, China  
e-mail: baoliwang@163.com

F. Wang (✉)  
Institute of Applied Radiation, School of Environmental and Chemical Engineering, Shanghai University, 333 Nanchen Road, Shanghai 200433, China  
e-mail: fswang@shu.edu.cn

X.-L. Liu · Z.-L. Wang  
Tianjin Key Laboratory of Water Resources and Environment, Tianjin Normal University, Tianjin 300387, China

1999). Unlike river acidification, ocean acidification is mainly due to the uptake of anthropogenic CO<sub>2</sub>, which is estimated to have caused a 30 % increase in the concentration of H<sup>+</sup> in ocean surface waters since the early 1900's (Raven et al. 2005). Yet, uptake of anthropogenic CO<sub>2</sub> by river waters seems to be impossible as CO<sub>2</sub> partial pressure in river waters is usually higher than that in the atmosphere (Mayorga et al. 2005; Wang et al. 2007). Obviously, there are other reasons inducing the pH decrease downstream from the hydroelectric dam.

Therefore, pH and related physical, chemical and biological variables were investigated monthly in a series of reservoirs along the Wujiang River, Southwest China. The purpose of this study is to understand the mechanism controlling pH variation in relation to the hydroelectric dam construction. This study may aid decision makers in determining sound management strategies for addressing hydropower exploitation in the future.

## Study area and methods

The Wujiang River is a southern tributary of the Changjiang River, with a length of 1037 km and a drainage area of  $8.8 \times 10^4$  km<sup>2</sup>. It is the largest river in Guizhou Province, with an average runoff of  $53.4 \times 10^9$  m<sup>3</sup> per year and a fall of 2,124 m. The Wujiang River basin is underlain dominantly by Permian and Triassic carbonate rocks (Han and Liu 2004). Over the past five decades, a series of reservoirs have been constructed along the Wujiang River (Fig. 1). The river is now a major hydropower source for China's massive West-to-East power transmission project.

For this study, water samples were collected monthly from July 2007 to June 2008 (Fig. 1). Water profiles were investigated in the Hongjiadu (W3), Dongfeng (W7), Wujiangdu (W15), Baihua (M8) and Hongfeng (M5) reservoirs. Surface water (upper 0.5 m) samples were collected from other stations. Water samples for depth profiles were taken with 5 L Niskin bottles. Sampling depths were 0, 5, 15, 30 and 60 m in the W3, W7 and W15; 0, 5, 10, 15 and 20 m in the M8, and 0, 3, 6, 10, 15 and 25 m in the M5 sampling locations.

Temperature (T), dissolved oxygen (DO), pH and chlorophyll were measured in situ using a calibrated water quality probe YSI 6600 V2 (YSI Inc., USA). In this study, mean pH was calculated using the geometric mean. Samples for major cation and anion analyses were filtered through 0.45 μm Sartorius® cellulose acetate filters. Cation samples were acidified to a pH of 2 with ultra-purified HNO<sub>3</sub>. Major cations (Ca<sup>2+</sup>, Mg<sup>2+</sup>, K<sup>+</sup> and Na<sup>+</sup>) were analyzed by inductively coupled plasma-optical emission spectrometry (ICP-OES; Vista MPX, Varian, Inc.) with a precision better than 5 %. Anions (SO<sub>4</sub><sup>2-</sup>, NO<sub>3</sub><sup>-</sup> and Cl<sup>-</sup>)

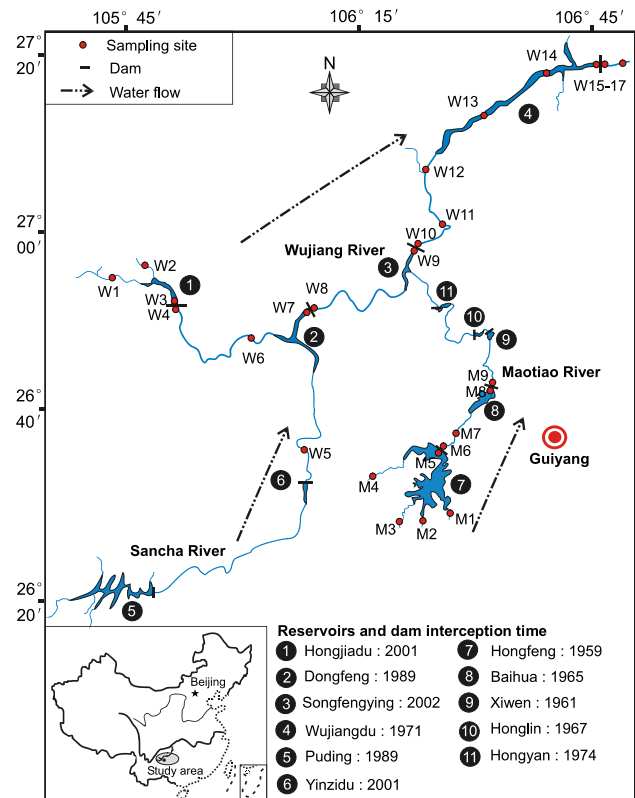
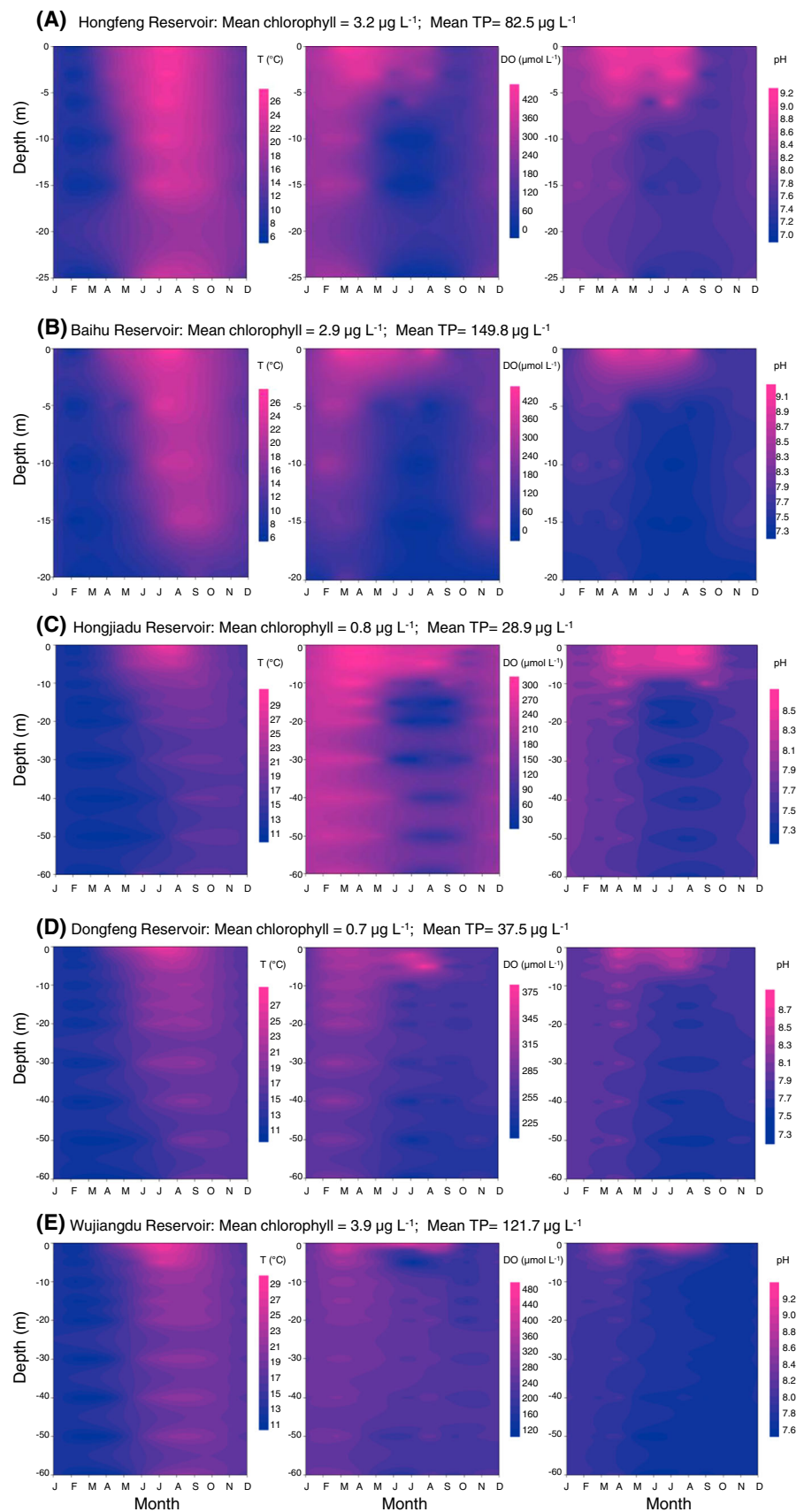


**Fig. 1** Map showing sampling locations and sample numbers. Water profiles were investigated in the Hongjiadu (W3), Dongfeng (W7), Wujiangdu (W15), Baihua (M8) and Hongfeng (M5) reservoirs and surface waters were collected from other stations

were determined by ion chromatography on a Dionex 120 with a precision of 5 %. Total phosphorus (TP) was analyzed spectrophotometrically (Unico UV-2000) after alkaline potassium persulfate digestion. Samples for dissolved organic carbon (DOC) analysis were filtered through pre-combusted 0.7 μm GF/F filters and were collected into pre-combusted brown glass vials. DOC was measured using wet chemical oxidation techniques and an OI Analytical Aurora 1030 TOC Analyzer. Total alkalinity (TA) was titrated with HCl in the field. An overpressure of CO<sub>2</sub> makes TA measurements in situ quite important. Concentrations of HCO<sub>3</sub><sup>-</sup>, CO<sub>3</sub><sup>2-</sup> and dissolved CO<sub>2</sub> (CO<sub>2</sub><sup>\*</sup>) were calculated based on TA, pH and T field data with equilibrium constants corrected for T and ionic strength (Barth and Veizer 1999; Maberly 1996). The calcite saturation index (SIc) was calculated as:  $SIc = \log \left( \frac{[Ca^{2+}][CO_3^{2-}]}{Kc} \right)$ , where Kc is corrected for T (Liu et al. 2008; Plummer and Busenberg 1982). The ionic strength was calculated from the major ions.

Samples for δ<sup>13</sup>C of dissolved inorganic carbon (δ<sup>13</sup>C<sub>DIC</sub>) measurements were collected by filtering 100 mL of water through 0.45 μm filters with a syringe into polyethylene vials, and then a saturated HgCl<sub>2</sub> solution

**Fig. 2** Monthly depth profiles of temperature (T), dissolved oxygen (DO) and pH in the five reservoirs. Means of chlorophyll and total phosphorus (TP) of each reservoir are also shown. See Fig. 1 for site locations



was injected into the vials for sample preservation. The vials were immediately closed without headspace with caps and sealed with seal film (Parafilm). In the laboratory, the sample was injected into closed evacuated glass vessels containing concentrated phosphoric acid and then heated at 50 °C to extract CO<sub>2</sub> (Atekwana and Krishnamurthy 1998). CO<sub>2</sub> was cryogenically separated and its pressure and temperature were measured in a sensor (Edwards Barocel<sup>®</sup> 600). The <sup>13</sup>C/<sup>12</sup>C ratio of CO<sub>2</sub> was determined on a dual-inlet isotope ratio mass spectrometer (MAT 252). Carbon isotope data were normalized and are reported following the “δ” denotation of Craig (1953) relative to the Vienna Pee Dee Belemnite (VPDB). The total precision for concentration and δ<sup>13</sup>C analysis were better than 3 % (1σ) and 0.1 % (1σ), respectively.

Pearson's correlation coefficient analyses were carried out with the software SPSS (version 11.5; SPSS, Inc.). Contour graphs were produced using Surfer (version 10; Golden Software Inc.).

## Results

The studied reservoirs showed a clear thermal, chemical and biological stratification from May to September (Fig. 2). The thermal stratification was accompanied by the development of hypoxia and acidification in the hypolimnion, which was inconspicuous during thermal homogeneity. Analysis of all data revealed a significant correlation between pH and O<sub>2</sub> concentration (Table 1), suggesting a strong linkage between pH decrease in the hypolimnion and the consumption of O<sub>2</sub>. The Hongfeng, Baihua and Wujiangdu reservoirs were eutrophic according to their chlorophyll and TP concentrations (Vollenweider and Kerekes 1982). The reservoirs with higher chlorophyll and TP concentrations had a greater pH difference (Δ pH) in their depth profiles (Fig. 2), and pH also showed a significant correlation with chlorophyll concentrations (Table 1).

**Table 1** Results of Pearson's correlation coefficient analysis

	DO	Chl	CO <sub>2</sub>	DIC	δ <sup>13</sup> C <sub>DIC</sub>	DOC
pH	0.658 <sup>a</sup>	0.522 <sup>a</sup>	−0.723 <sup>a</sup>	−0.450 <sup>a</sup>	0.544 <sup>a</sup>	0.170 <sup>a</sup>
DO		0.400 <sup>a</sup>	−0.473 <sup>a</sup>	−0.150 <sup>a</sup>	0.312 <sup>a</sup>	0.008
Chl			−0.203 <sup>a</sup>	−0.156 <sup>a</sup>	0.345 <sup>a</sup>	0.177 <sup>a</sup>
CO <sub>2</sub>				0.590 <sup>a</sup>	−0.302 <sup>a</sup>	−0.035
DIC					−0.379 <sup>a</sup>	−0.051
δ <sup>13</sup> C <sub>DIC</sub>						0.303 <sup>a</sup>

DO dissolved oxygen, Chl chlorophyll, CO<sub>2</sub> dissolved CO<sub>2</sub>, DIC dissolved inorganic carbon, DOC dissolved organic carbon

<sup>a</sup> Correlation is significant at the 0.01 level (2-tailed)

The reservoir waters had a higher pH than the releasing water (i.e., waters downstream from the dams), and significant differences for pH between upstream and downstream of the dam were observed (one-way ANOVA,  $P < 0.05$ ; Fig. 3). The main Wujiang channel showed up to a 0.47 pH decrease from upstream to downstream of the dam in the Wujiangdu Reservoir, while its branch at the Maotiao River had up to a 0.41 pH decrease in the Hongfeng Reservoir. However, reservoir waters had similar mean pH values to each other as well as to the entering waters in the Wujiangdu Reservoir (sites W11–15), although pH differences in this reservoir were relatively high (Fig. 3).

Study results showed that pH had significant positive correlations to δ<sup>13</sup>C<sub>DIC</sub> and DOC (Table 1), suggesting an effect of the carbon biogeochemical cycle on pH variation. HCO<sub>3</sub><sup>−</sup> was the predominant carbon species of dissolved inorganic carbon (DIC), with a mean contribution of 94.5 % (Table 2). pH increased with decreases in CO<sub>2</sub><sup>\*</sup> and increases in CO<sub>3</sub><sup>2−</sup>, while DIC and TA decreased slightly with increases in pH (Fig. 4). TA showed similar values as DIC, and the ratio of TA to DIC was constrained to 1 ( $r = 0.96$  and  $p < 0.001$ ).

## Discussion

Carbon biogeochemical cycle in relation to pH variation

Dam construction for hydropower usually creates deep reservoirs and, therefore, the resulting impounded waters may gradually develop physical, chemical and biological stratifications. As illustrated in the conceptual model (Fig. 5), study findings show that vertical coupling between photosynthesis in the epilimnion and respiration in the hypolimnion was largely responsible for the negative correlation between CO<sub>2</sub><sup>\*</sup> and O<sub>2</sub>. Photosynthesis mainly occurred in the surface water, consuming lighter CO<sub>2</sub> and making the δ<sup>13</sup>C of residual DIC more positive than −8.5 ‰ (i.e., the δ<sup>13</sup>C of DIC from carbonate dissolution, Peng et al. 2014). When O<sub>2</sub> is available, aerobic respiration occurs in the subsurface waters, that is (CH<sub>2</sub>O)<sub>106</sub>(NH<sub>3</sub>)<sub>16</sub>H<sub>3</sub>PO<sub>4</sub> + 138O<sub>2</sub> → 106CO<sub>2</sub> + 16HNO<sub>3</sub> + H<sub>3</sub>PO<sub>4</sub> + 122H<sub>2</sub>O. The production of a small amount of the strong acid, HNO<sub>3</sub>, plays a minor role in reducing pH and TA (Cai et al. 2011), while the hydration of CO<sub>2</sub> led to an significant increase in the DIC pool. Moreover, the inputs of respiratory CO<sub>2</sub> resulted in the δ<sup>13</sup>C of DIC pool more negative than −8.5 ‰. At the sediment–water interface, anaerobic respiration via NO<sub>3</sub><sup>−</sup> consumption can occur when O<sub>2</sub> is sufficiently low (Fig. 5); however, the net result of anaerobic respiration on CO<sub>2</sub> parameters is similar to that of aerobic respiration (Canfield

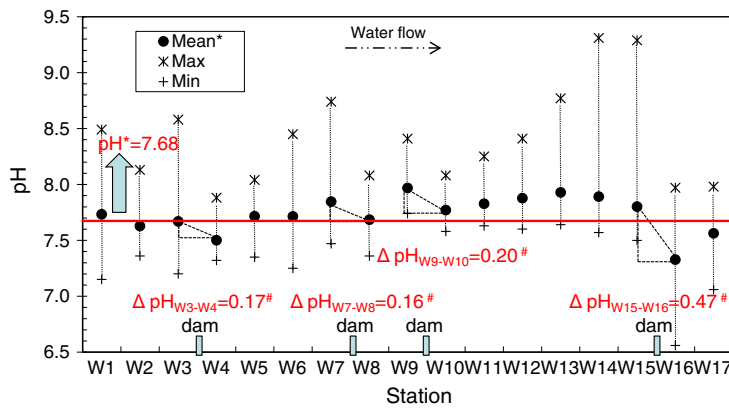


**Fig. 3** pH variation in the Wujiang main channel and its branch of the Maotiao River. The pH differences from upstream to downstream of a dam in each reservoir were calculated from the mean pH. See

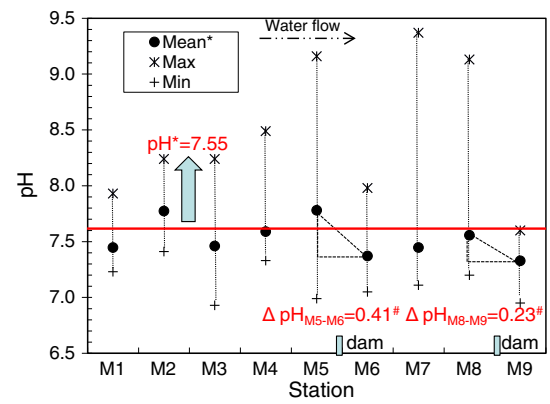


**Fig. 1** for site locations. Asterisks Mean calculated from the geometric mean. Hash Mean pH difference was significant from upstream to downstream of a dam (one-way ANOVA,  $P < 0.05$ )

**Table 2** Physical and chemical parameters relating to the carbonate equilibria in this study. The calculations are based on all the data

Parameter	Mean	SD	Min	Max
Temperature (°C)	16.4	5.3	5.5	30.2
pH	7.67 <sup>a</sup>	0.42	6.56	9.37
TA ( $\mu\text{mol L}^{-1}$ )	2,273.8	354.9	1,167.3	4,049.7
DIC ( $\mu\text{mol L}^{-1}$ )	2,377.2	416.8	1,109.0	4,589.6
$\text{HCO}_3^-$ ( $\mu\text{mol L}^{-1}$ )	2,245.8	366.7	1,054.4	4,042.5
$\text{CO}_2^*$ ( $\mu\text{mol L}^{-1}$ )	118.0	116.8	1.3	1,388.9
$\text{CO}_3^{2-}$ ( $\mu\text{mol L}^{-1}$ )	13.4	23.5	0.5	256.8
DOC ( $\mu\text{mol L}^{-1}$ )	203.2	123.3	28.4	1,107.1
$\delta^{13}\text{C}_{\text{DIC}}$ (‰)	-8.1	1.5	-12.9	-1.3

The arithmetic average of pH was 7.83

TA total alkalinity, DIC dissolved inorganic carbon, DOC dissolved organic carbon

<sup>a</sup> Mean calculated from the geometric mean

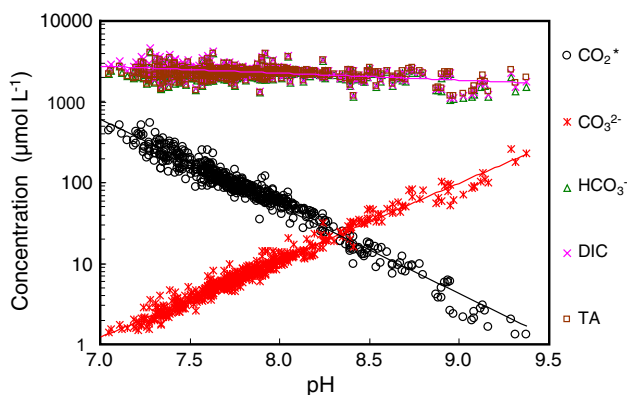


**Fig. 4** Scatter plots of pH versus total alkalinity (TA), DIC,  $\text{HCO}_3^-$ ,  $\text{CO}_2^*$  and  $\text{CO}_3^{2-}$ , respectively, for the total dataset

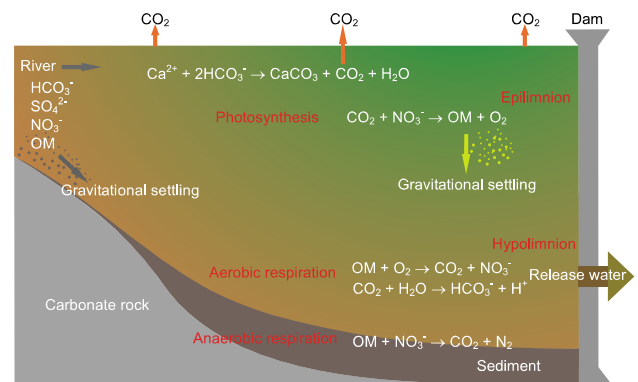


**Fig. 5** A sketch map for carbon biogeochemical cycle in a reservoir. OM organic matter

et al. 1993; Hu and Cai 2011). The evidence from  $\delta^{13}\text{C}_{\text{DIC}}$  indicated photosynthesis and respiration significantly influenced the pH variation (Fig. 6). According to correlation analyses, it was negligible for the inputs of respiratory  $\text{CO}_2$  from the DOC to DIC pool, and DOC has a limited impact on pH in this study.

$\text{NO}_3^-$  was involved in the vertical carbon biogeochemical cycle. As for the reservoirs in the Wujiang main channel,  $\text{CO}_2^*$  and  $\text{NO}_3^-$  exhibited significant correlations in the depth profiles ( $r = 0.47$  and  $p < 0.001$ ), while this phenomenon was not found in the reservoirs in its branch at the Maotiao River. Based on this correlation analysis, only aerobic respiration occurred in the hypolimnion of the reservoirs in the Wujiang main channel, while in its branch at the Maotiao River, additional anaerobic respiration also happened due to hypoxia ( $[\text{O}_2] < 62.5 \mu\text{mol L}^{-1}$ ) at the bottom (Canfield et al. 1993; Hu and Cai 2011). This shift from aerobic to anaerobic respiration changed the

**Fig. 6** Scatter plot of pH versus  $\delta^{13}\text{C}_{\text{DIC}}$  in the depth profiles of the five reservoirs. See Fig. 1 for site locations

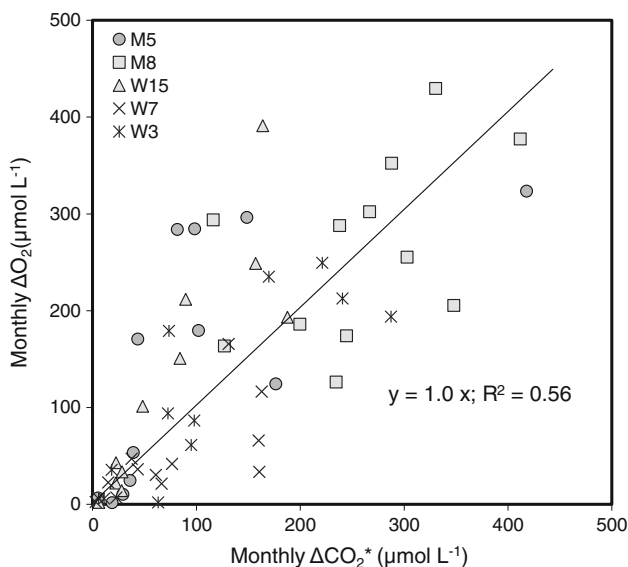
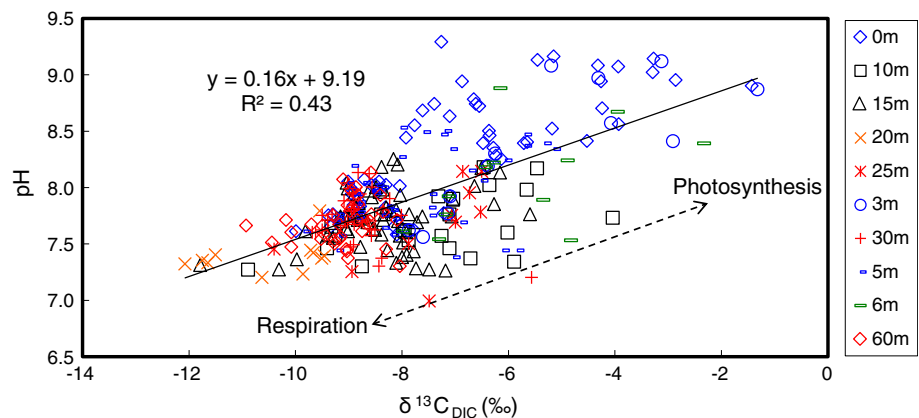


**Fig. 7** Scatter plot of monthly  $\text{O}_2$  difference ( $\Delta\text{O}_2$ , Max–Min) versus monthly  $\text{CO}_2^*$  difference ( $\Delta\text{CO}_2^*$ , Max–Min) in the depth profiles of the five reservoirs. See Fig. 1 for site locations

stoichiometric ratio of  $\text{CO}_2^*$  and  $\text{NO}_3^-$ , and finally resulted in the decoupling of  $\text{CO}_2^*$  and  $\text{NO}_3^-$  at the bottom.

There is a stoichiometric relationship between  $\text{O}_2$  and  $\text{CO}_2$  in the processes of photosynthesis and respiration. According to the respiration equation, this stoichiometric ratio of  $\text{O}_2$  to  $\text{CO}_2$  is 1.3. The similar differences between  $\text{CO}_2^*$  and  $\text{O}_2$  in the depth profiles indicated that the molar rate of photosynthetic synthesis of organic carbon in the epilimnion was similar to that of respiratory decomposition of organic carbon in the hypolimnion (Fig. 7). Therefore, pH increases in the surface and associated pH decreases in the subsurface may counteract each other if there is no additional  $\text{CO}_2$  input. This appears to be the reason that the mean pH in the Wujiangdu Reservoir showed a similar value to that in the entering river water (Fig. 3).

#### Mechanism controlling pH decrease downstream from a dam

If the river water is considered to be an ideal carbonate solution, then the following relationships can be applied:  $\text{TA} - \text{DIC} = [\text{CO}_3^{2-}] - [\text{CO}_2]$ , and  $\text{pH} = -0.5 \log(K_1 K_2) - 0.5 \log([\text{CO}_2]/[\text{CO}_3^{2-}])$ , where  $K_1$  and  $K_2$  are dissociation constants of the carbonic acid. Then, at the point where  $\text{DIC} = \text{TA}$ , a slight increase in  $\text{CO}_2$  and an associated decrease in  $\text{CO}_3^{2-}$  will cause a large decrease in pH. As the Wujiang River watershed has a karstic geological substrate, the river water chemistry is mainly controlled by carbonate weathering (Chetelat et al. 2008; Han and Liu 2004). Therefore, the Wujiang River is an ideal bicarbonate buffering system where  $\text{DIC} \approx \text{TA}$  (Fig. 4). In depth profiles, an increase in pH in the surface was caused by a lower  $[\text{CO}_2]/[\text{CO}_3^{2-}]$  ratio, while conversely a decrease in pH in the subsurface resulted from a higher  $[\text{CO}_2]/[\text{CO}_3^{2-}]$  ratio (Fig. 8a). In addition, the increase of algal biomass enhanced  $\Delta\text{pH}$  in depth profiles in response to enhanced photosynthesis in the epilimnion and respiration in the hypolimnion (Fig. 9). Calcium carbonate is usually present in concentrations at supersaturation in the studied river waters (Wang et al. 2011); however, this study found that the pH decrease changed the calcium carbonate saturation state and resulted in undersaturation due to the decrease of  $\text{CO}_3^{2-}$  at the bottom (Fig. 8b).

Most reservoirs employ deep water introduction for power generation (Fig. 5). This operation of releasing bottom waters decreases the pH downstream from a dam. This decrease along with an associated change in the calcite saturation state may have profound influences on the river ecosystem (Burns et al. 2008; Merz-Preiß and Riding 1999). The increase in sulfur and nitrogen levels in the Wujiang River (Chen et al. 2002; Han and Liu 2004) could also induce the acidification of river waters. This external forcing toward acidification may be reduced by the

**Fig. 8** Scatter plots of pH versus  $[CO_2^*]/[CO_3^{2-}]$  ratio (a) and calcite saturation index (SIc) (b) in the depth profiles of the five reservoirs. See Fig. 1 for site locations

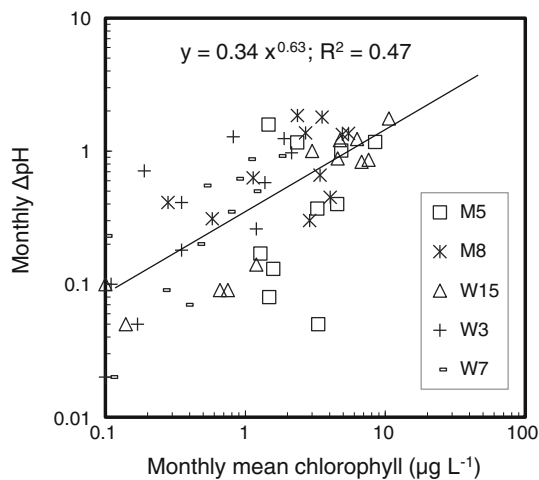
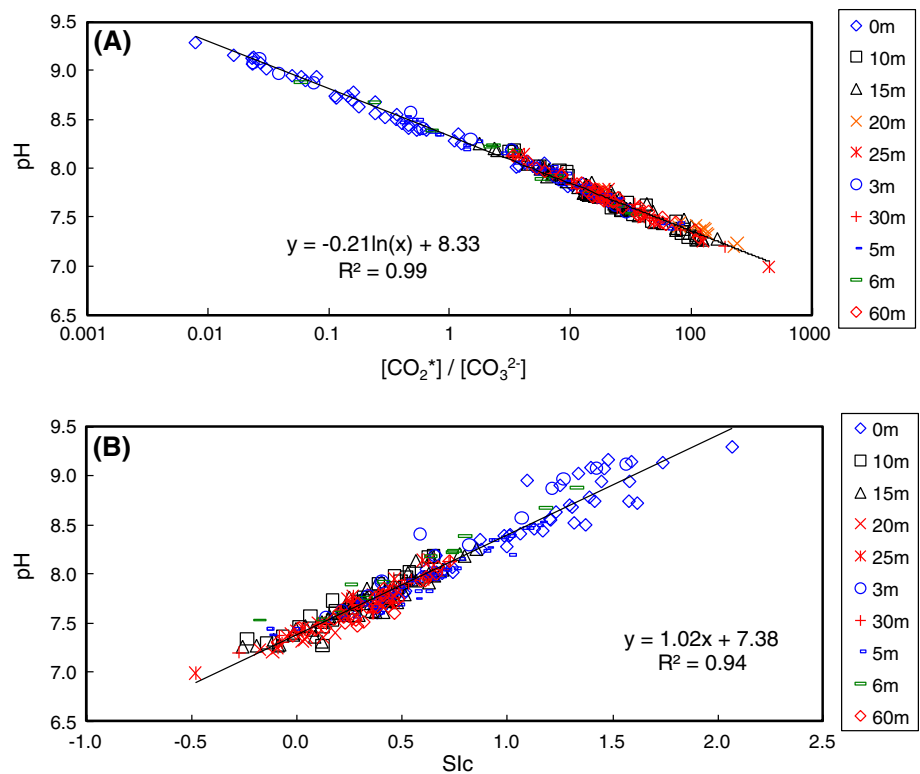


**Fig. 9** Scatter plot of monthly pH difference ( $\Delta pH$ , Max–Min) versus monthly mean of chlorophyll in the depth profiles of the five reservoirs. See Fig. 1 for site locations

bicarbonate buffering system. However, this buffering cannot reduce river acidification downstream from the associated dam, which is controlled by the carbon biogeochemical cycle. Although there is serious pH decrease downstream from the hydroelectric dam, the releasing waters will gradually recover their pH as they flow further away from the dam due to the degassing of  $CO_2$  in the surface water.

**Conclusions**

A series of dam constructions on the Wujiang River has disrupted this river continuum, and its associated impounded waters have developed physical, chemical and biological stratifications. As the Wujiang River is an ideal bicarbonate buffering system, study findings showed that the pH in this impounded river was mainly controlled by  $[CO_2]/[CO_3^{2-}]$  ratios. Photosynthesis induced a lower  $[CO_2]/[CO_3^{2-}]$  ratio in the surface while respiration induced a higher  $[CO_2]/[CO_3^{2-}]$  ratio in the subsurface. This finally led to significant pH differences in the water profile, and the evidence from  $\delta^{13}C_{DIC}$  clearly demonstrated these processes. The operation of releasing bottom water for power generation decreased the pH downstream from the dam, and the average drop in pH from upstream to downstream of a dam was up to 0.47 units. The excessive production of phytoplankton enhanced this pH decrease, while DOC had limited impacts on this pH variation. The cascade in hydropower development could increase the risk of river acidification.

**Acknowledgments** We are grateful to Ganrong Li, Zhiwei Han and Chipeng Zhang for their assistance in sample collection in the field. This study was financially supported by the Foundation of Chinese Academy of Sciences (Grant Nos: kzcx2-ew-102), National Key Basic Research Program of China (Grant No: 2013CB956703) and National Natural Science Foundation of China (Grant Nos. 41021062 and 41173096).

## References

- Atekwana EA, Krishnamurthy RV (1998) Seasonal variations of dissolved inorganic carbon and  $\delta^{13}\text{C}$  of surface water: application of a modified gas evolution technique. *J Hydrol* 205:265–278
- Barth JAC, Veizer J (1999) Carbon cycle in St. Lawrence aquatic ecosystems at Cornwall (Ontario), Canada: seasonal and spatial variations. *Chem Geol* 159:107–128
- Burns DA, Riva-Murray K, Bode RW, Passy S (2008) Changes in stream chemistry and biology in response to reduced levels of acid deposition during 1987–2003 in the Neversink River Basin, Catskill Mountains. *Ecol Indic* 8:191–203
- Cai WJ, Hu X, Huang WJ, Murrell MC, Lehrter JC, Lohrenz SE, Chou WC, Zhai W et al (2011) Acidification of subsurface coastal waters enhanced by eutrophication. *Nat Geosci* 4:766–770
- Canfield DE, Jorgensen BB, Fossing H, Glud R, Gundersen J, Ramsing NB, Thamdrup B, Hansen JW et al (1993) Pathways of organic carbon oxidation in the three continental margin sediments. *Mar Geol* 113:27–40
- Chen J, Wang F, Xia X, Zhang L (2002) Major element chemistry of the Changjiang (Yangtze River). *Chem Geol* 187:231–255
- Chetelat B, Liu CQ, Zhao ZQ, Wang QL, Li SL, Li J, Wang B (2008) Geochemistry of the dissolved load of the Changjiang Basin rivers: anthropogenic impacts and chemical weathering. *Geochim Cosmochim Acta* 72:4254–4277
- Craig H (1953) The geochemistry of stable carbon isotopes. *Geochim Cosmochim Acta* 3:53–92
- Duan L, Ma X, Larssen T, Mulder J, Hao J (2011) Response of surface water acidification in upper Yangtze River to  $\text{SO}_2$  emissions abatement in China. *Environ Sci Technol* 45:3275–3281
- Han G, Liu CQ (2004) Water geochemistry controlled by carbonate dissolution: a study of the river waters draining karst-dominated terrain, Guizhou Province, China. *Chem Geol* 204:1–21
- Hu X, Cai WJ (2011) An assessment of ocean margin anaerobic processes on oceanic alkalinity budget. *Global Biogeochem Cycles* 25:GB3003
- Humborg C, Ittekkot V, Cociasu A, Bodungen BV (1997) Effect of Danube river dam on Black Sea biogeochemistry and ecosystem structure. *Nature* 386:385–388
- Larssen T, Lydersen E, Tang DG, He Y, Gao JX, Liu HY, Duan L, Seip HM et al (2006) Acid rain in China. *Environ Sci Technol* 40:418–425
- Liu Z, Liu X, Liao C (2008) Daytime deposition and nighttime dissolution of calcium carbonate controlled by submerged plants in a karst spring-fed pool: insights from high time-resolution monitoring of physico-chemistry of water. *Environ Geol* 55:1159–1168
- Maberly SC (1996) Diel, episodic and seasonal changes in pH and concentration of inorganic carbon in a productive lake. *Freshw Biol* 35:579–598
- Mayorga E, Aufdenkampe AK, Masiello CA, Krusche AV, Hedges JI, Quay PD, Richey JE, Brown TA (2005) Young organic matter as a source of carbon dioxide outgassing from Amazonian rivers. *Nature* 436:538–541
- Merz-Preiß M, Riding R (1999) Cyanobacterial tufa calcification in two freshwater streams: ambient environment, chemical thresholds and biological processes. *Sediment Geol* 126:103–124
- Peng X, Liu CQ, Wang B, Zhao YC (2014) The impact of damming on geochemical behavior of dissolved inorganic carbon in a karst river. *Chin Sci Bull* 59:2348–2355
- Plummer LN, Busenberg E (1982) The solubilities of calcite, aragonite, and vaterite in  $\text{CO}_2$ - $\text{H}_2\text{O}$  solutions between 0 and 90°C and an evaluation of the aqueous model for the system  $\text{CaCO}_3$ - $\text{CO}_2$ - $\text{H}_2\text{O}$ . *Geochim Cosmochim Acta* 46:1011–1040
- Raven J, Caldeira K, Elderfield H, Hoegh-Guldberg O, Liss P, Riebesell U, Shepherd J, Turley C et al (2005) Ocean acidification due to increasing atmospheric carbon dioxide. The Royal Society, London
- Stoddard JL, Jeffries DS, Lukewille A, Clair TA, Dillon PJ, Driscoll CT, Forsius M, Johannessen M et al (1999) Regional trends in aquatic recovery from acidification in North America and Europe. *Nature* 401:575–578
- Vollenweider RA, Kerekes J (1982) Eutrophication of waters: monitoring assessment and control. Organization for Economic Co-Operation and Development (OECD), Paris, p 156
- Vörösmarty CJ, Sharma KP, Fekete BM, Copeland AH, Holden J, Marble J, Lough JA (1997) The storage and aging of continental runoff in large reservoir systems of the world. *Ambio* 26:210–219
- Wang F, Wang Y, Zhang J, Xu H, Wei X (2007) Human impact on the historical change of  $\text{CO}_2$  degassing flux in River Changjiang. *Geochem Trans* 8:7
- Wang F, Wang B, Liu CQ, Wang Y, Guan J, Liu X, Yu Y (2011) Carbon dioxide emission from surface water in cascade reservoirs–river system on the Maotiao river, southwest of China. *Atmos Environ* 45:3827–3834
- Wang B, Liu CQ, Peng X, Wang F (2013) Mechanisms controlling the carbon stable isotope composition of phytoplankton in karst reservoirs. *J Limnol* 72:127–139
- Wang F, Liu CQ, Wang B, Yu Y, Liu X (2014) Influence of a reservoir chain on the transport of riverine inorganic carbon in the karst area. *Environ Earth Sci* 72:1465–1477